Journal of Information Systems Engineering and Management
2024, 9 (4)
e-ISSN: 2468-4376
https://www.jisem-journal.com/

Research Article

Lipid Concentration Effects on Blood Flow through Inclined Stenosed Tube Experiencing Body Acceleration and Slip Velocity

Dr. Neha Phogat[1*], Prof. Sumeet Gill[2], Dr. Rajbala Rathee[3]
[1 *]Assistant Professor (On Contract), Deptt. of Mathematics, M.D. University, Rohtak-124001, Haryana, India
[2] Professor, Deptt. of Mathematics, M. D. University, Rohtak-124001, Haryana, India
[3] Assistant Professor, A.I.J.H. Memorial College, Rohtak-124001, Haryana, India

ARTICLE INFO

Received: 10 Sep 2024

Accepted: 24 Dec 2024

ABSTRACT

The present investigation delves into the intricate interplay between a magnetic field and slip velocity in the context of blood flow through inclined stenosed artery with permeable walls. In this analysis, blood is regarded as an elastic-viscous fluid, and the study explores the impact of temperature and concentration on the flow of blood. To solve the complex non-linear coupled equations governing this phenomenon, the Homotopy Perturbation Method is employed. The results are then visually presented through the utilization of MATLAB Programming. In this comprehensive study, particular attention is given to the influence of Brownian Motion Parameters and Thermophoresis Parameters. Transformation methods are appropriately applied to compute crucial parameters such as axial velocity, volumetric flow rate, and shear stress. These computations are carried out within a cylindrical polar coordinate system. This research contributes a novel perspective on the understanding of various parameters governing blood flow characteristics and circulation within the human body under the influence of a magnetic field and slip velocity. Furthermore, the investigation extends its scope to encompass the dimension of body acceleration, shedding light on how it interacts with the aforementioned factors to influence blood circulation in inclined stenosed arteries with permeable walls.

KEYWORDS: Elastic-viscous fluid, Slip velocity, Wall permeability, Transverse magnetic field, Brownian motion, Thermophoresis.

Introduction

The study explores the dynamic interplay between lipid concentrations and blood flow within an inclined stenosed tube, subject to both body acceleration and slip velocity. The circulatory system, a vital conduit for sustaining human life, faces intricate challenges, and understanding the impact of lipid concentrations becomes pivotal in elucidating the complexities of hemodynamics. Stenosis, a narrowing of arterial passages, further complicates the landscape, demanding a thorough investigation into its repercussions on blood flow characteristics. The unique aspects of this analysis lie in its incorporation of body acceleration, and the consideration of slip velocity, acknowledging the interaction between blood and the vessel walls. As lipid concentrations assume a central role in atherosclerotic processes, this chapter aims to unravel their effects on key hemodynamic parameters, offering insights into the alterations of shear stress, pressure profiles, and velocity distributions within the inclined stenosed tube. Through a comprehensive approach encompassing mathematical modeling, numerical simulations, and analytical scrutiny, the study contributes to the understanding of cardiovascular dynamics.

Omamoke and Amos [1] studied the theoretical effects of body acceleration and slip parameter on unsteady blood flow by assuming blood as non-newtonian fluid flowing through stenosed artery. Further, Amos et al. [2] developed a mathematical model to show the effects of magnetic field and slip parameter on blood flowing through inclined stenosed artery. Padma et al. [3] derived the solutions for velocity, shear stress and flow resistance to analyze the

Copyright © 2024 by Author/s and Licensed by JISEM. This is an open access article distributed under the Creative Commons Attribution License which permitsunrestricted use, distribution, and reproduction in any medium, provided the original work is properly cited.

Journal of Information Systems Engineering and Management
2024, 9 (4)
e-ISSN: 2468-4376
https://www.jisem-journal.com/

Research Article

blood flow analysis in the presence of magnetic field. Das et al. [4] explained the rheological behavior of blood by focusing on flow characteristics in the porous medium using Homotopy Perturbation Method.

Formulation of the Problem

We considered blood as a "Non-Newtonian Elastico-viscous", "incompressible" and electrically conducting fluid with nano-particles under the influence of transversely applied "magnetic field". Motion of blood is assumed to be one-dimensional in a straight and rigid cylindrical stenosed artery through a porous medium. Further, the blood flow is assumed to be "laminar, unsteady, axially-symmetric and fully developed". The cylindrical coordinate system (r, z) is considered such that velocity component along z axis is u. "Heat and mass transfer phenomenon" is calculated by assigning temperature T and concentration C to the wall of the tube.
The geometry of an inclined stenosed artery is shown in figure 1 as proposed by Srivastava [5].

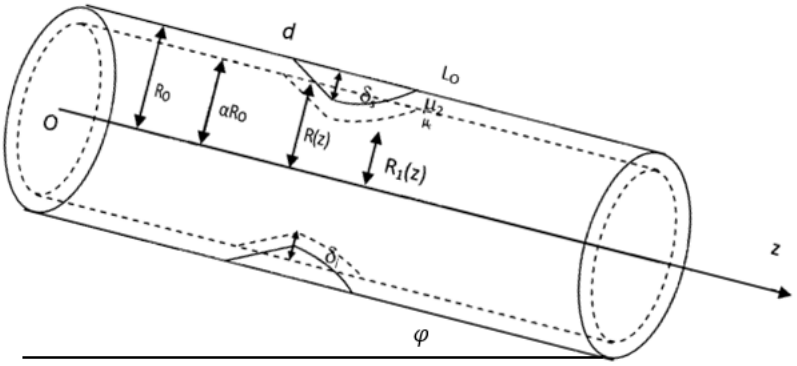


Figure 1

$$\frac{R(z)}{R_o(z)} = 1 - F[l_o^{n-1}(z-d) - (z-d)^n]\ ; d \le z \le d + l_o \qquad (1)$$

where, $n \ge 2$ is the parameter determining the "shape of stenosis" for which the "symmetric stenosis" is found for $n = 2$, d is the "position of stenosis", l_o is the "length of stenosis", $R_o(z)$ expresses the radius of unstenosed artery, $R(z)$ is the "radius of circular cylindrical stenosed artery", z indicates the "axial position" and the parameter F is given by $F = \frac{\varepsilon}{R_o l_o^n}\frac{n^{n/(n-1)}}{(n-1)}$; ε is the maximum height of developed stenosis which is located at $z = d + \frac{l_o}{n^{1/(n-1)}}$; $\frac{\varepsilon}{R_o(z)} \ll 1$.

Now, the equations governing the flow in cylindrical polar co-ordinates are:

$$\mu\nabla^2 u + \mu_1\frac{\partial}{\partial t'}(\nabla^2 u) - \sigma\beta_o^2 u \quad \frac{p}{z} \quad \frac{\mu}{K}u \quad g(\rho\gamma)_{nf}(T \quad T) \quad \rho g\tilde{\alpha}(C \quad C) + \rho g\, Sin\varphi + \rho G(t) \quad \rho\frac{u}{t'} \qquad (2)$$

$$\frac{1}{(\rho C_p)_{nf}}\, Q_0 + \alpha_{nf}\,\frac{1}{r}\left[\frac{\partial}{\partial r}\left(r\frac{\partial T}{\partial r}\right)\right] + \zeta\left[D_B\left(\frac{\partial C}{\partial r}\right)\left(\frac{\partial T}{\partial r}\right) + \frac{D_T}{T_0}\left(\frac{\partial T}{\partial r}\right)^2\right] = \frac{\partial T}{\partial t'} \qquad (3)$$

and

$$D_B\left[\frac{1}{r}\frac{\partial}{\partial r}\left(r\frac{\partial C}{\partial r}\right)\right] + \frac{D_T}{T_0}\left[\frac{1}{r}\frac{\partial}{\partial r}\left(r\frac{\partial T}{\partial r}\right)\right] = \frac{\partial C}{\partial t'} \qquad (4)$$

where $\nabla^2 = \frac{1}{r}\frac{\partial}{\partial r}\left(r\frac{\partial}{\partial r}\right)$, $G(t) = G_0 Cos(w_b t + \phi)$, G_0 represents the amplitude of body acceleration, $w_b = 2\pi f_b$, f_b is the body acceleration frequency, ϕ is the phase difference, $\frac{p}{z} = A_o + A_1\cos(t/t_o)$, A_o is the "constant amplitude of pressure gradient", A_1 is the "amplitude of the pulsatile component", $1/t_o = 2\pi f_p$, f_p is the "heart pulse frequency", t' is the time variable, T is the temperature, C is concentration, $u(r, t')$ is the "axial velocity component", ρ is the "density

Copyright © 2024 by Author/s and Licensed by JISEM. This is an open access article distributed under the Creative Commons Attribution License which permitsunrestricted use, distribution, and reproduction in any medium, provided the original work is properly cited.

Journal of Information Systems Engineering and Management
2024, 9 (4)
e-ISSN: 2468-4376
https://www.jisem-journal.com/

Research Article

of blood", μ is the "viscosity of blood", μ_1 is "elastic viscosity coefficient of blood", g is the acceleration due to gravity, $\zeta = \frac{(\rho C)_{nf}}{(\rho C)_f}$ is the ratio between the "effective heat capacity of nano particle" and "heat capacity of the fluid", K is the "permeability of the isotropic porous medium", D_B is the Brownian diffusion coefficient, D_T is the thermospheric diffusion coefficient and r is the radial co-ordinate.
The boundary conditions are as follows:

$$\frac{\partial C}{\partial r} = 0 \text{ when } r = 0 \quad (5)$$

$$C = C_o \text{ when } r = R(z) \quad (6)$$

$$\frac{\partial T}{\partial r} = 0 \text{ when } r = 0 \quad (7)$$

$$T = T_o \text{ when } r = R(z) \quad (8)$$

Defining,

$$T = \left[\tilde{\theta} + 1\right]T_o \ ; \ C = [\tilde{\sigma} + 1]C_o \ ; \ t' = tt_o \ ; \ r = yR_o \quad (9)$$

The non-dimensional forms are as follows:

$$\left[1 + \psi\frac{\partial}{\partial t}\right]\nabla^2 u \quad M^2 u + N(A_o + A_1 \cos t) \quad H^2 u \quad G_r\tilde{\theta} \quad G_f\tilde{\sigma} + g_0 + G_0 Cos(bt + \phi) \quad \alpha^2\frac{u}{t} \quad (10)$$

$$\nabla^2\tilde{\theta} \quad \beta \quad N_B\frac{\tilde{\sigma}}{y}\frac{\tilde{\theta}}{y} \quad N_T\left(\frac{\tilde{\theta}}{y}\right)^2 \quad \frac{1}{\alpha_1^2}\frac{\tilde{\theta}}{t} \quad (11)$$

and

$$\nabla^2\tilde{\sigma} \quad \left(\frac{N_T}{N_B}\right)\nabla^2\tilde{\theta} \quad \frac{1}{\alpha_2^2}\frac{\tilde{\sigma}}{t} \quad (12)$$

where $\nabla^2 \quad \frac{1}{y}\frac{}{y}\left(y\frac{}{y}\right), \beta \quad \frac{Q\,R^2}{\alpha_{nf}T\,(\rho C_p)_{nf}}, \quad \frac{p}{z} = A_o + A_1\cos t, \beta \quad \frac{Q\,R^2}{\alpha_{nf}T\,(\rho C_p)_{nf}},$

$N_B \quad C\,\frac{\zeta D_B}{\alpha_{nf}}$ is the "Brownian motion parameter", $N_T \quad \zeta\frac{D_T}{\alpha_{nf}}$ is the "thermospheric parameter", $\alpha_1^2 \quad \frac{\alpha_{nf}t}{R^2}$, $\alpha_2^2 \quad \frac{D_B t}{R^2}$, $\psi = \frac{\mu_1}{\mu t_o}$, $M = \beta_o R_o\sqrt{\frac{\tilde{\sigma}}{\mu}}$ is the "Hartmann number", $H = R_o\sqrt{\frac{1}{K}}$ is the permeability parameter, $\alpha = R_o\sqrt{\frac{\rho}{\mu t_o}}$ is the Womersley parameter , $N = \frac{R_o^2}{\mu}$, $G_r = g(\rho\gamma)_{nf}\frac{R_0^2 T_o}{\mu}$ is the local temperature Grashof number, $G_f = g\rho\alpha\frac{C_o R_o^2}{\mu}$ is the local Grashof number and $g_0 = \frac{R_0^2\rho g Sin\varphi}{\mu}$.

Further, it is assumed that for values of $t < 0$, only heart's pumping action exists and for $t = 0$, artery's blood flow leads to the "instant pressure gradient" i.e.

$$-\frac{\partial p}{\partial z} = A_o + A_1 \quad (13)$$

The boundary conditions in the non-dimensional form are as follows:

$$\frac{\partial\tilde{\theta}}{\partial y} = 0 \text{ when } y = 0 \quad (14)$$

$$\tilde{\theta} = 0 \text{ when } y = R(z) \quad (15)$$

$$\frac{\partial\tilde{\sigma}}{\partial y} = 0 \text{ when } y = 0 \quad (16)$$

$$\tilde{\sigma} = 0 \text{ when } y = R(z) \quad (17)$$

The initial condition is described as

$$u' + hu = 0 \text{ when } r = a \text{ and } t \geq 0 \quad (18)$$

where $h = -\frac{\eta}{R_o\sqrt{K}}$ and $a = \frac{R(z)}{R_o(z)}$; η is constant which depends on the properties of "porous medium" and on its structure.

Copyright © 2024 by Author/s and Licensed by JISEM. This is an open access article distributed under the Creative Commons Attribution License which permitsunrestricted use, distribution, and reproduction in any medium, provided the original work is properly cited.

Journal of Information Systems Engineering and Management
2024, 9 (4)
e-ISSN: 2468-4376
https://www.jisem-journal.com/

Research Article

Solution of the Problem

The solution of the non-linear coupled equations (11) and (12) are calculated by constructing homotopies and applying "Homotopy Perturbation technique" as follows:

$$H(i,\tilde{\theta}) = (1-i)[L(\tilde{\theta}) - L(\tilde{\theta}_{10})] + i\left[L(\tilde{\theta}) + \beta \quad N_B \frac{\tilde{\sigma}}{y}\frac{\tilde{\theta}}{y} \quad N_T\left(\frac{\tilde{\theta}}{y}\right)^2 - \frac{1}{\alpha_1^2}\frac{\tilde{\theta}}{t}\right] \tag{19}$$

$$H(i,\tilde{\sigma}) = (1-i)[L(\tilde{\sigma}) - L(\tilde{\sigma}_{10})] + i\left[L(\tilde{\theta}) + \left(\frac{N_T}{N_B}\right)\frac{1}{y}\frac{}{y}\left(y\frac{\tilde{\theta}}{y}\right) - \frac{1}{\alpha_2^2}\frac{\tilde{\sigma}}{t}\right] \tag{20}$$

where i is the embedding parameter with range $0 \le i \le 1$; $L = \frac{1}{y}\frac{}{y}\left(y\frac{}{y}\right)$ is a linear operator ; $\tilde{\theta}_{10}$ and $\tilde{\sigma}_{10}$ are the initial approximations.

Now, let the initial approximations as follows:

$$\tilde{\theta}_{10}(y,z) = -\frac{(y^2-R^2)}{4}e^{\omega t} \tag{21}$$

$$\tilde{\sigma}_{10}(y,z) = -\frac{(y^2-R^2)}{4}e^{\omega t} \tag{22}$$

where ω is constant.

Define,

$$\tilde{\theta} = \tilde{\theta}_o + i\tilde{\theta}_1 + o(i)^2 \tag{23}$$

$$\tilde{\sigma} = \tilde{\sigma}_o + i\tilde{\sigma}_1 + o(i)^2 \tag{24}$$

On solving (19) and (20) by using (23) and (24), we get

$$\tilde{\theta}(y,t) = \frac{(y^2-R^2)}{4}\beta - (N_T+N_B)e^{2\omega t}\frac{(y^4-R^4)}{64} - \frac{(y^4-R^4)}{64}\frac{\omega e^{\omega t}}{\alpha_1^2} + \frac{(y^2-R^2)}{16}\frac{R^2\omega e^{\omega t}}{\alpha_1^2} \tag{25}$$

and

$$\tilde{\sigma}(y,t) = \frac{N_T}{N_B}\frac{(y^2-R^2)}{4}e^{\omega t} - \frac{(y^4-R^4)}{64}\frac{\omega e^{\omega t}}{\alpha_2^2} + \frac{(y^2-R^2)}{16}\frac{R^2\omega e^{\omega t}}{\alpha_2^2} \tag{26}$$

Putting (25) and (26) in equation (10) and using Laplace transformation, Hankel transformation, Laplace inverse transformation and Hankel inverse transformation, we get

$$\begin{aligned}
u(y,t) = {} & \frac{2}{a^2}\sum_{n=1}^{\infty}\frac{\lambda_n^2}{(h^2+\lambda_n^2)}\frac{J_o(y\lambda_n)}{J_o^2(a\lambda_n)}\left[\left[\frac{N(A_o+A_1)+g_0+G_0\,Cos\,\phi}{(M^2+H^2+\lambda_n^2)}\left(e^{-Bt}\right)\right.\right. \\
& \left.\left.+\frac{NA_o+g_0}{B(\alpha^2+\psi\lambda_n^2)}(1-e^{-Bt})\right]\left[\frac{a}{\lambda_n}J_1(a\lambda_n)\right] + \left[\frac{NA_1}{(\alpha^2+\psi\lambda_n^2)}\left\{\frac{B}{(1+B^2)}\left(\cos t + \frac{1}{B}\sin t - e^{-Bt}\right)\right\}\right]\times \\
& \left[\frac{a}{\lambda_n}J_1(a\lambda_n)\right] + \left[\frac{G_0\,Cos\,\phi}{(\alpha^2+\psi\lambda_n^2)}\left(\frac{1}{(b^2+B^2)}\right)(B\cos t + b\sin bt - Be^{-Bt})\right]\left[\frac{a}{\lambda_n}J_1(a\lambda_n)\right] \\
& -\left[\frac{G_0\,b\,Sin\,\phi}{(\alpha^2+\psi\lambda_n^2)}\left(\frac{1}{(b^2+B^2)}\right)\left(\frac{B}{b}\,Sinbt - \cos bt + e^{-Bt}\right)\right]\left[\frac{a}{\lambda_n}J_1(a\lambda_n)\right] \\
& -\frac{e^{-Bt}}{(M^2+H^2+\lambda_n^2)}\left(G_rN_T + G_rN_B + \frac{\omega}{\alpha_1^2}G_r + \frac{\omega}{\alpha_2^2}G_f\right)\left(\left(\frac{a^4-R^4}{64}\right)\frac{a}{\lambda_n}J_1(\lambda_n a)\right. \\
& \left.-\frac{3a^4}{64\lambda_n^2}J_2(\lambda_n a) + \frac{3a^3}{32\lambda_n^3}J_3(\lambda_n a)\right) + \frac{e^{-Bt}}{(M^2+H^2+\lambda_n^2)}\left(\beta G_r + \frac{R^2\omega}{4\alpha_1^2}G_r + \frac{N_T}{N_B}G_f + \frac{R^2\omega}{4\alpha_2^2}G_f\right)\times \\
& \left(\left(\frac{a^2-R^2}{4}\right)\frac{a}{\lambda_n}J_1(\lambda_n a) - \frac{a^2}{2\lambda_n^2}J_2(\lambda_n a)\right) + \frac{G_r}{(\alpha^2+\psi\lambda_n^2)}\left(\left[\frac{-(N_T+N_B)\left(e^{2\omega t}-e^{-Bt}\right)}{(B+2\omega)}\right.\right. \\
& \left.\left.-\frac{\omega\left(e^{\omega t}-e^{-Bt}\right)}{\alpha_1^2(B+\omega)}\right]\left[\left(\frac{a^4-R^4}{64}\right)\frac{a}{\lambda_n}J_1(\lambda_n a) - \frac{3a^4}{64\lambda_n^2}J_2(\lambda_n a) + \frac{3a^3}{32\lambda_n^3}J_3(\lambda_n a)\right]\right. \\
& +\frac{R^2\omega\left(e^{\omega t}-e^{-Bt}\right)}{4\alpha_1^2(B+\omega)}\left[\left(\frac{a^2-R^2}{4}\right)\frac{a}{\lambda_n}J_1(\lambda_n a) - \frac{a^2}{2\lambda_n^2}J_2(\lambda_n a)\right] \\
& \left.+\frac{\beta(1-e^{-Bt})}{B}\left[\left(\frac{a^2-R^2}{4}\right)\frac{a}{\lambda_n}J_1(\lambda_n a) - \frac{a^2}{2\lambda_n^2}J_2(\lambda_n a)\right]\right) \\
& +\frac{G_f}{(\alpha^2+\psi\lambda_n^2)}\frac{\left(e^{\omega t}-e^{-Bt}\right)}{(B+\omega)}\left(\left[\frac{N_T}{N_B}+\frac{R^2w}{4\alpha_2^2}\right]\left[\left(\frac{a^2-R^2}{4}\right)\frac{a}{\lambda_n}J_1(\lambda_n a) - \frac{a^2}{2\lambda_n^2}J_2(\lambda_n a)\right]\right. \\
& \left.\left.-\frac{\omega}{\alpha_2^2}\left[\left(\frac{a^4-R^4}{64}\right)\frac{a}{\lambda_n}J_1(\lambda_n a) - \frac{3a^4}{64\lambda_n^2}J_2(\lambda_n a) + \frac{3a^3}{32\lambda_n^3}J_3(\lambda_n a)\right]\right)\right]
\end{aligned} \tag{27}$$

The expression for the volumetric flow rate is given by

Copyright © 2024 by Author/s and Licensed by JISEM. This is an open access article distributed under the Creative Commons Attribution License which permitsunrestricted use, distribution, and reproduction in any medium, provided the original work is properly cited.

Journal of Information Systems Engineering and Management
2024, 9 (4)
e-ISSN: 2468-4376
https://www.jisem-journal.com/

Research Article

$$Q(y,t)=\frac{4\pi}{a}\sum_{n=1}^{\infty}\frac{\lambda_n}{(h^2+\lambda_n^2)}\frac{J_1(a\lambda_n)}{J_o^2(a\lambda_n)}\left[\left[\frac{N(A_o+A_1)+g_0+G_0\,Cos\,\phi}{(M^2+H^2+\lambda_n^2)}\left(e^{-Bt}\right)\right.\right.$$
$$\left.+\frac{NA_o+g_0}{B(\alpha^2+\psi\lambda_n^2)}\left(1-e^{-Bt}\right)\right]\left[\frac{a}{\lambda_n}J_1(a\lambda_n)\right]+\left[\frac{NA_1}{(\alpha^2+\psi\lambda_n^2)}\left\{\frac{B}{(1+B^2)}\left(\cos t+\frac{1}{B}\sin t-e^{-Bt}\right)\right\}\right]\times$$
$$\left[\frac{a}{\lambda_n}J_1(a\lambda_n)\right]+\left[\frac{G_0\,Cos\,\phi}{(\alpha^2+\psi\lambda_n^2)}\left(\frac{1}{(b^2+B^2)}\right)\left(B\cos t+b\sin bt-Be^{-Bt}\right)\right]\left[\frac{a}{\lambda_n}J_1(a\lambda_n)\right]$$
$$-\left[\frac{G_0\,b\,Sin\,\phi}{(\alpha^2+\psi\lambda_n^2)}\left(\frac{1}{(b^2+B^2)}\right)\left(\frac{B}{b}\,Sinbt-\,cos\,bt+e^{-Bt}\right)\right]\left[\frac{a}{\lambda_n}J_1(a\lambda_n)\right]$$
$$-\frac{e^{-Bt}}{(M^2+H^2+\lambda_n^2)}\left(G_rN_T+G_rN_B+\frac{\omega}{\alpha_1^2}G_r+\frac{\omega}{\alpha_2^2}G_f\right)\left(\left(\frac{a^4-R^4}{64}\right)\frac{a}{\lambda_n}J_1(\lambda_na)\right.$$
$$\left.-\frac{3a^4}{64\lambda_n^2}J_2(\lambda_na)+\frac{3a^3}{32\lambda_n^3}J_3(\lambda_na)\right)+\frac{e^{-Bt}}{(M^2+H^2+\lambda_n^2)}\left(\beta G_r+\frac{R^2\omega}{4\alpha_1^2}G_r+\frac{N_T}{N_B}G_f+\frac{R^2\omega}{4\alpha_2^2}G_f\right)\times$$
$$\left(\left(\frac{a^2-R^2}{4}\right)\frac{a}{\lambda_n}J_1(\lambda_na)-\frac{a^2}{2\lambda_n^2}J_2(\lambda_na)\right)+\frac{G_r}{(\alpha^2+\psi\lambda_n^2)}\left(\left[\frac{-(N_T+N_B)\left(e^{2\omega t}-e^{-Bt}\right)}{(B+2\omega)}\right.\right.$$
$$\left.-\frac{\omega\left(e^{\omega t}-e^{-Bt}\right)}{\alpha_1^2(B+\omega)}\right]\left[\left(\frac{a^4-R^4}{64}\right)\frac{a}{\lambda_n}J_1(\lambda_na)-\frac{3a^4}{64\lambda_n^2}J_2(\lambda_na)+\frac{3a^3}{32\lambda_n^3}J_3(\lambda_na)\right]$$
$$+\frac{R^2\omega\left(e^{\omega t}-e^{-Bt}\right)}{4\alpha_1^2(B+\omega)}\left[\left(\frac{a^2-R^2}{4}\right)\frac{a}{\lambda_n}J_1(\lambda_na)-\frac{a^2}{2\lambda_n^2}J_2(\lambda_na)\right]$$
$$\left.+\frac{\beta\left(1-e^{-Bt}\right)}{B}\left[\left(\frac{a^2-R^2}{4}\right)\frac{a}{\lambda_n}J_1(\lambda_na)-\frac{a^2}{2\lambda_n^2}J_2(\lambda_na)\right]\right)$$
$$+\frac{G_f}{(\alpha^2+\psi\lambda_n^2)}\frac{\left(e^{\omega t}-e^{-Bt}\right)}{(B+\omega)}\left(\left[\frac{N_T}{N_B}+\frac{R^2w}{4\alpha_2^2}\right]\left[\left(\frac{a^2-R^2}{4}\right)\frac{a}{\lambda_n}J_1(\lambda_na)-\frac{a^2}{2\lambda_n^2}J_2(\lambda_na)\right]\right.$$
$$\left.\left.-\frac{\omega}{\alpha_2^2}\left[\left(\frac{a^4-R^4}{64}\right)\frac{a}{\lambda_n}J_1(\lambda_na)-\frac{3a^4}{64\lambda_n^2}J_2(\lambda_na)+\frac{3a^3}{32\lambda_n^3}J_3(\lambda_na)\right]\right)\right] \tag{28}$$

Graphical Discussion

Numerical experiments have been conducted and graphical analysis is done for axial velocity and for volumetric flow rate. Figure 2 to 5 show the behaviour of axial velocity for different parameters along the axial distance. In figure 2, axial velocity decreases with increasing values of magnetic field. Figure 3 reveals that axial velocity increases with increasing slip parameter. The figure 4 shows that the axial velocity rises with growth in body acceleration. Figure 5 emphasizes that the axial velocity decreases when arterial inclination angle increases.

Figure 6 to 10 exhibit the behaviour of volumetric flow rate with different parameters. From the figures it can be observed that the volumetric flow rate behaves in the similar manner as reflected by the axial velocity in correspondence to different parameters. Figure 10 illustrates that the volumetric flow rate diminishes with low lipid concentration and rising nanoparticle concentration. Conversely, at elevated levels of both lipid and nanoparticle concentrations, the volumetric flow rate exhibits an increase. Elevated blood flow can potentially strain the cardiovascular system, leading to increased stress on the heart and blood vessels.

Copyright © 2024 by Author/s and Licensed by JISEM. This is an open access article distributed under the Creative Commons Attribution License which permitsunrestricted use, distribution, and reproduction in any medium, provided the original work is properly cited.

Journal of Information Systems Engineering and Management
2024, 9 (4)
e-ISSN: 2468-4376
https://www.jisem-journal.com/

Research Article

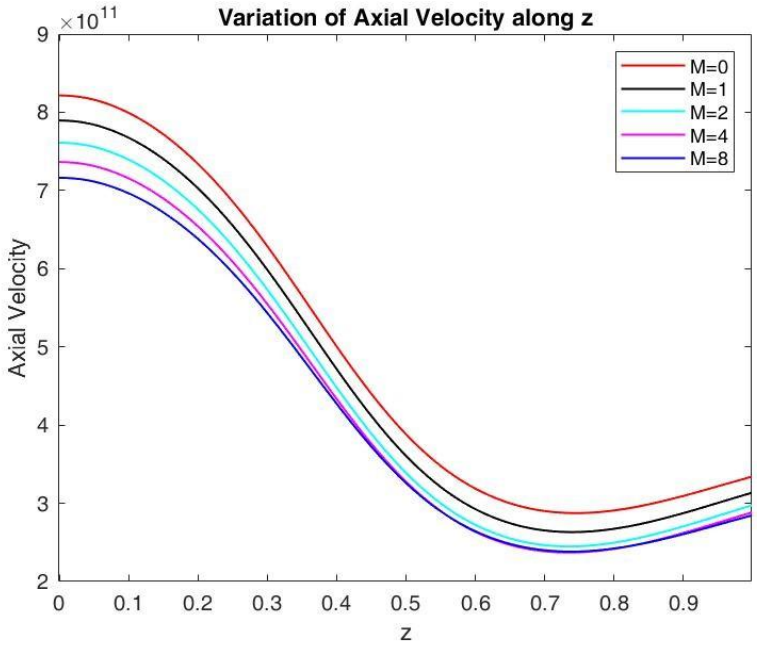


Figure 2

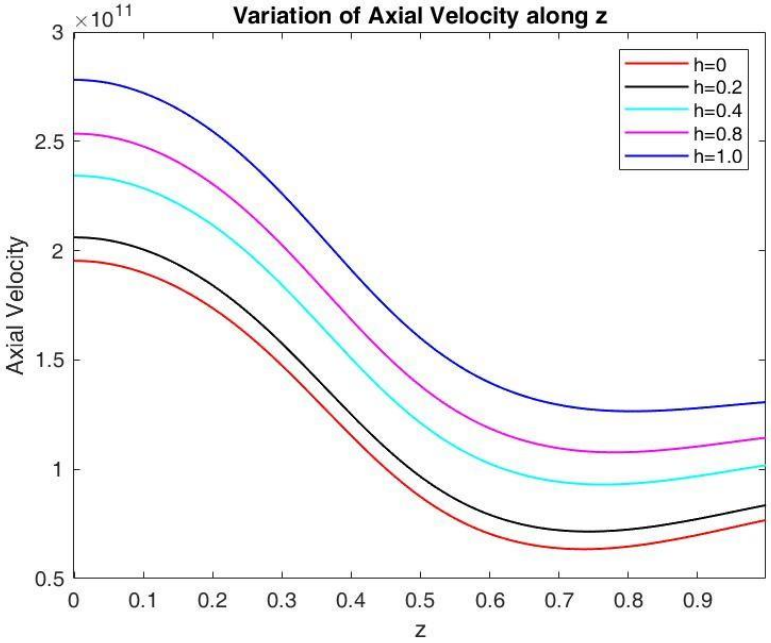


Figure 3

Copyright © 2024 by Author/s and Licensed by JISEM. This is an open access article distributed under the Creative Commons Attribution License which permitsunrestricted use, distribution, and reproduction in any medium, provided the original work is properly cited.

Journal of Information Systems Engineering and Management
2024, 9 (4)
e-ISSN: 2468-4376
https://www.jisem-journal.com/

Research Article

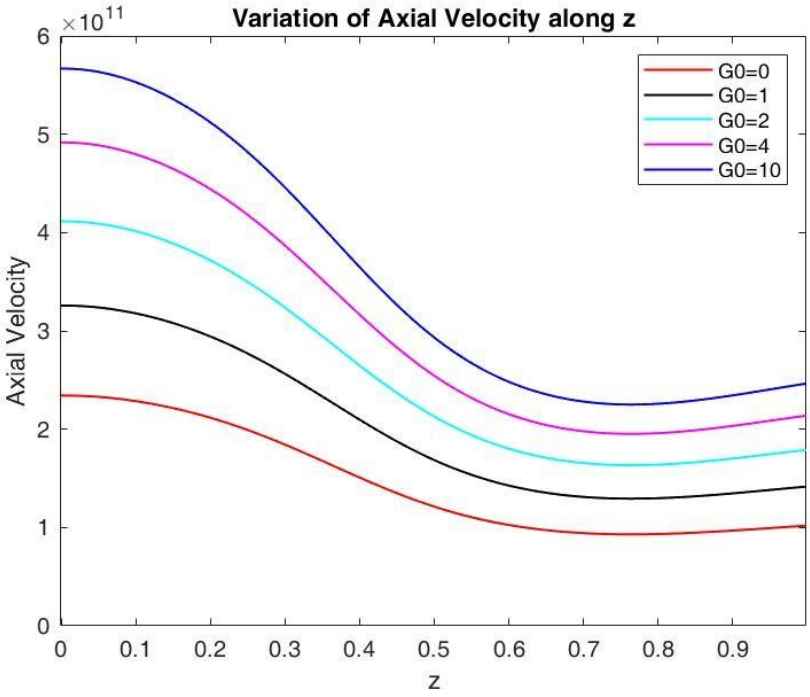


Figure 4

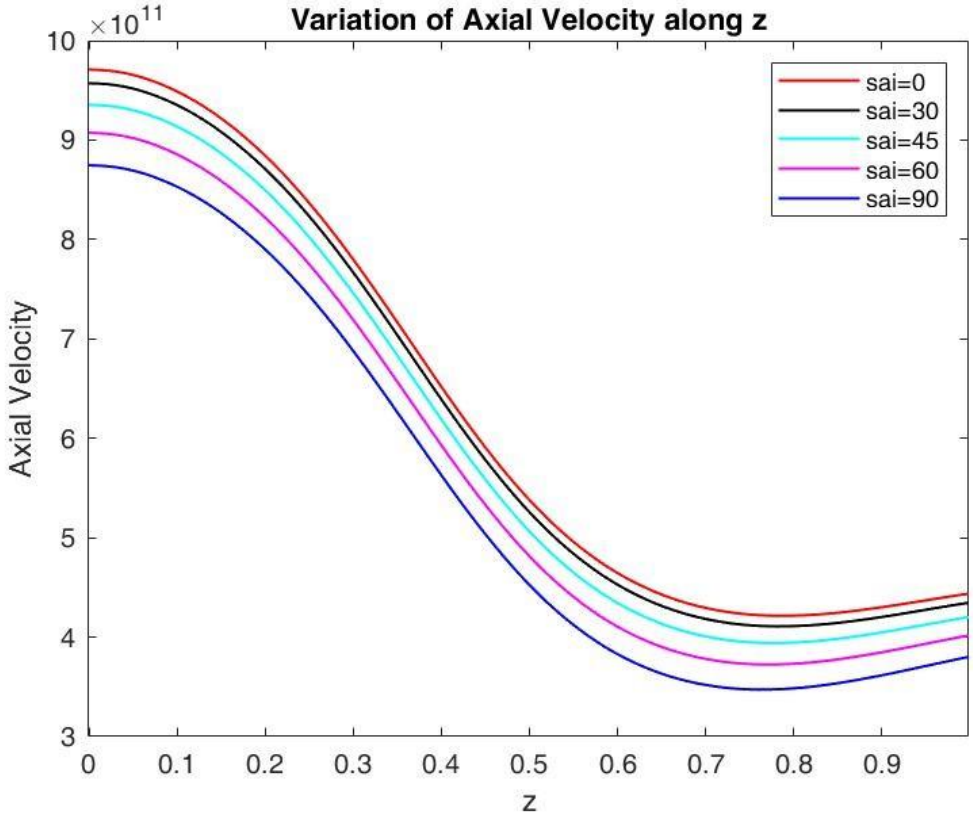


Figure 5

Copyright © 2024 by Author/s and Licensed by JISEM. This is an open access article distributed under the Creative Commons Attribution License which permitsunrestricted use, distribution, and reproduction in any medium, provided the original work is properly cited.

Journal of Information Systems Engineering and Management
2024, 9 (4)
e-ISSN: 2468-4376
https://www.jisem-journal.com/

Research Article

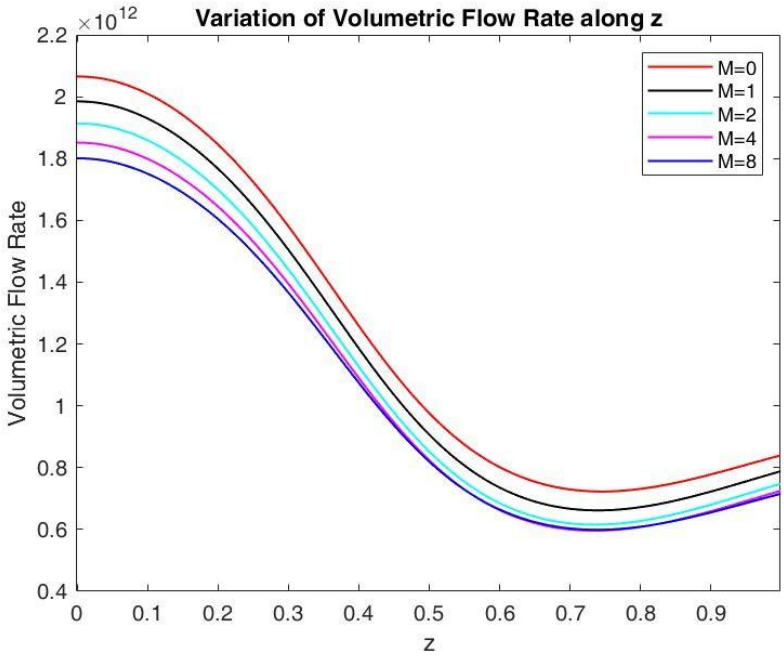


Figure 6

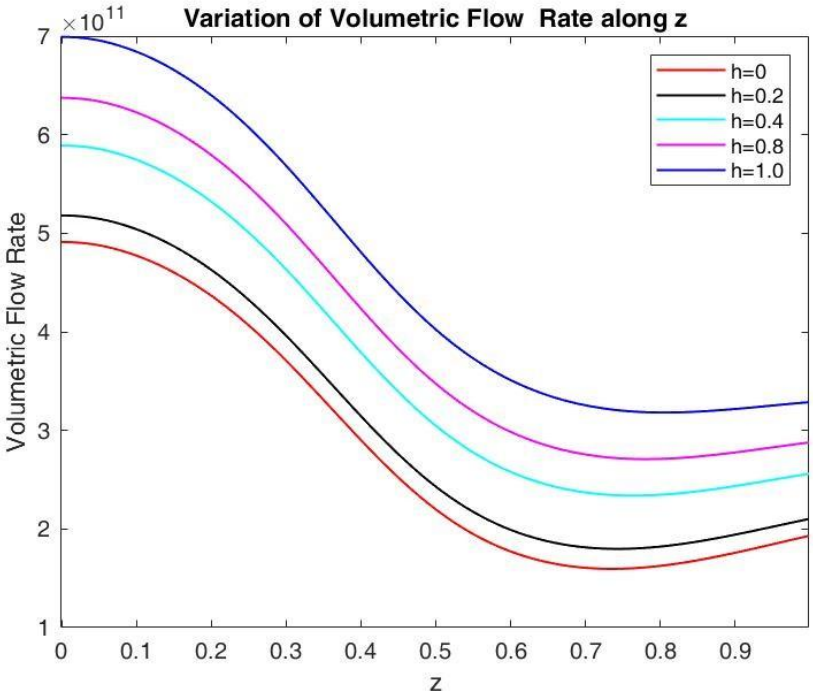


Figure 7

Copyright © 2024 by Author/s and Licensed by JISEM. This is an open access article distributed under the Creative Commons Attribution License which permitsunrestricted use, distribution, and reproduction in any medium, provided the original work is properly cited.

Journal of Information Systems Engineering and Management
2024, 9 (4)
e-ISSN: 2468-4376
https://www.jisem-journal.com/

Research Article

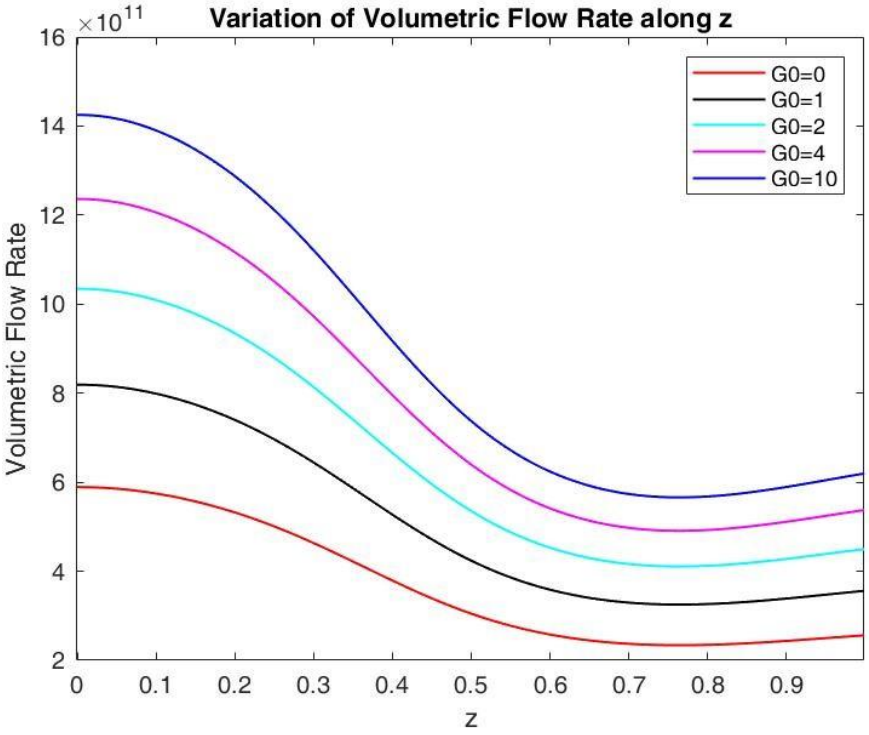


Figure 8

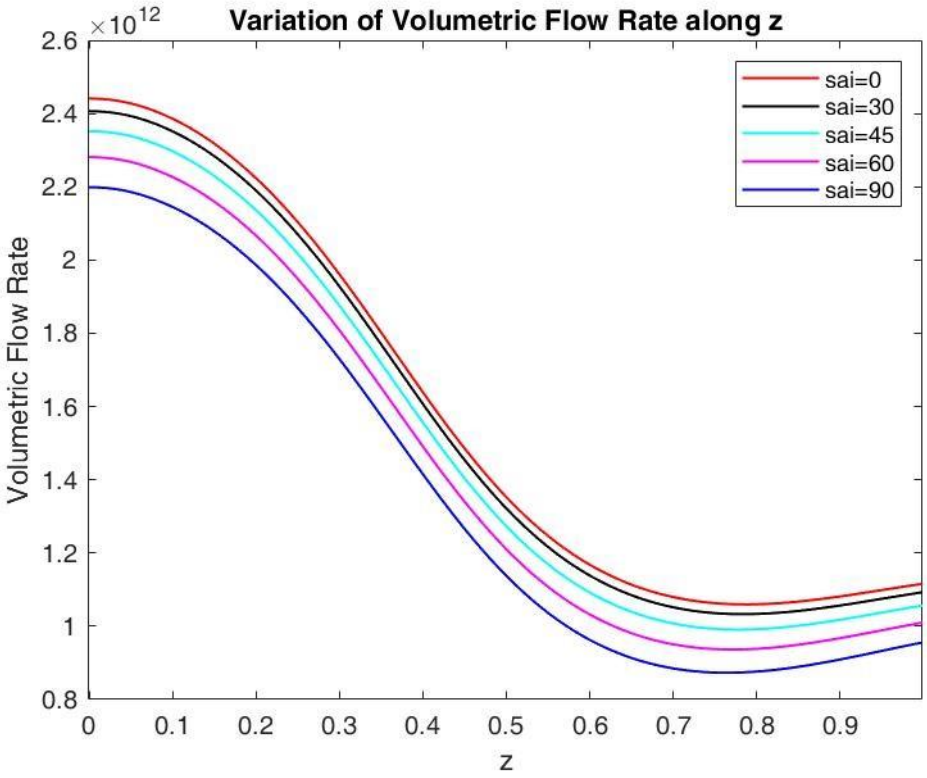


Figure 9

Copyright © 2024 by Author/s and Licensed by JISEM. This is an open access article distributed under the Creative Commons Attribution License which permitsunrestricted use, distribution, and reproduction in any medium, provided the original work is properly cited.

Journal of Information Systems Engineering and Management
2024, 9 (4)
e-ISSN: 2468-4376
https://www.jisem-journal.com/

Research Article

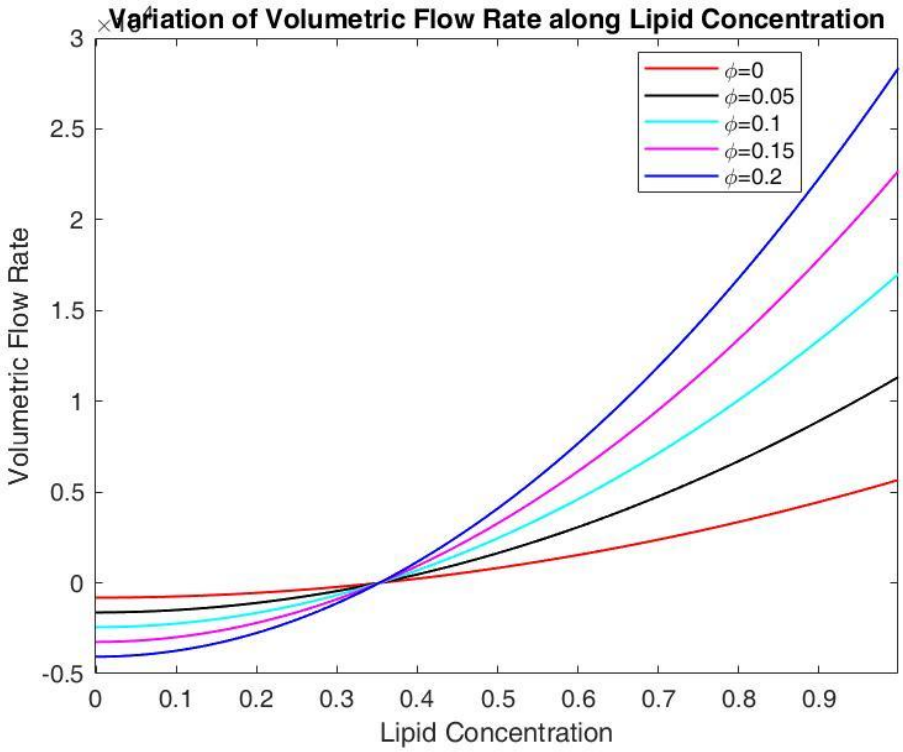


Figure 10

Conclusion

- Decreasing axial velocity due to high strength of magnetic field and arterial inclination angle can be controlled by regulated variation in values of slip parameter and body acceleration.
- Lower axial velocity might disturb the flow pattern in blood vessels which can cause shear stress on vessel walls.
- The observed correlation between lipid concentration, nanoparticle concentration, and volumetric flow rate in blood circulation can adversely impact cardiovascular health. Insufficient blood flow can lead to inadequate oxygen and nutrient delivery to tissues and organs, potentially causing tissue damage, organ dysfunction, and compromised overall health.

References

[1] Omamoke, E., & Amos, E. (2022). Slip and Pulsatile MHD Blood Flow Through An Inclined Stenosed Artery With Body Acceleration And Heat Source Effects. *IOSR Journal of Mathematics (IOSR-JM)*, 18(1): 01-23.
[2] Amos, E., Omamoke, E., & Nwaigwe, C. (2022). MHD pulsatile blood flow through an inclined stenosed artery with body acceleration and slip effects. *International Journal of Theoretical and Applied Mathematics*, 8(1): 1-3.
[3] Padma, R., Selvi, R. T., & Ponalagusamy, R. (2019). Effects of slip and magnetic field on the pulsatile flow of a Jeffrey fluid with magnetic nanoparticles in a stenosed artery. *The European Physical Journal Plus*, 134(5): 221.
[4] Das, S., Pal, T. K., & Jana, R. N. (2021). Outlining impact of hybrid composition of nanoparticles suspended in blood flowing in an inclined stenosed artery under magnetic field orientation. *BioNanoScience*, 11: 99-115.
[5] Srivastava V. P. (2000). Particulate suspension blood flow through stenotic arteries: effect of haematocrit and stenosis. *Indian J. Pure Appl. Math.*, 33: 1353-1360

Copyright © 2024 by Author/s and Licensed by JISEM. This is an open access article distributed under the Creative Commons Attribution License which permitsunrestricted use, distribution, and reproduction in any medium, provided the original work is properly cited.